Desalination and Water Treatment
www.deswater.com

doi: 10.5004/dwt.2017.20474

70 (2017) 175–182
April

Synthesis and use of nanomagnetic MnO_2 adsorbent for removing Pb(II) and Cd(II) ions from acid aqueous solutions

Carlos Basualto[a,*], Pablo González[a], Alejandro Briso[a], Kamila Barrera[a], Viviana Ide[a], Mireya Araya[a], Gonzalo Montes-Atenas[b], Fernando Valenzuela[a]

[a]*Laboratorio de Operaciones Unitarias, Facultad de Ciencias Químicas y Farmacéuticas, Universidad de Chile, Santos Dumont 964, Independencia, Santiago, Chile, emails: cbasualt@uchile.cl (C. Basualto), crams99@gmail.com (P. Gonzalez), alejandro.briso@gmail.com (A. Briso), kamiii.lee@gmail.com (K. Barrera), vivaracha@gmail.com (V. Ide), luthien1387@gmail.com (M. Araya), fvalenzu@uchile.cl (F. Valenzuela)*

[b]*Minerals and Metals Characterisation and Separation (M2SC) Research Group, Departamento de Ingeniería de Minas, Facultad de Ciencias Físicas y Matemáticas, Universidad de Chile, Av. Tupper 2069, Santiago, Chile, email: gmontes@ing.uchile.cl*

Received 11 August 2016; Accepted 27 December 2016

ABSTRACT

A nanoadsorbent based on δ-MnO_2 and Fe_3O_4 was synthesized and assessed as an adsorbent for removing some heavy metals from acidic aqueous solution. The δ-MnO_2 adsorbent was prepared in aqueous alkaline medium using an oxidative precipitation methodology in presence of superparamagnetic magnetite particles previously synthesized. The adsorbent was chemically, physically and magnetically characterized using several analytical techniques. The resulting adsorbent consists of nanoparticles with sizes below 1 μm forming larger agglomerated structures with a mean size ranging between 6 and 9 nm. The nanoparticles have superparamagnetic properties that allow separating the metal-loaded sorbent particles from the treated aqueous solution using conventional magnets. Pb(II) and Cd(II) adsorption tests were carried out showing that the metals adsorption increases with the pH of the aqueous solution, which is consistent with the observed adsorbent zeta potential measurements. Pb(II) and Cd(II) equilibrium experiments were conducted, and the results were studied using Langmuir and Freundlich isotherm models. Adsorption kinetics experiments were carried out separately for both metallic ions. A pseudo-second-order adsorption kinetics model explained well the experimental data.

Keywords: Magnetic adsorbent; MnO_2; Nanoparticles; Toxic ions; Adsorption; Removal

1. Introduction

In Chile, one of the major environmental problems concerning the management of liquids in mining-related activities is the generation of acid wastewaters triggered by chemical and/or microbial oxidation of sulfides in presence of air and water and produced by either hydrometallurgical processes or the natural generation of acid mine drainages (AMD) generated in tailing dumps. [1–3]. These mining aqueous solutions exhibit an important amount of chemical contaminants, either dissolved or suspended, at concentrations that normally surpass the maximum limits established by the Chilean national discharge regulations [4]. Water requirements in the mining industry are becoming a real problem, especially in regions such as the Atacama Desert or the Andes mountains, where this vital resource is scarce. Limited water resources ought to meet the needs of local communities as well as those related to the mining activities. Therefore, it is absolutely necessary to optimize the use of all the available water resources and, simultaneously, to control adequately the water composition according to its use particularly those close to human consumption and there pollutants rise as a major concern.

* Corresponding author.

Among the main pollutants found in acidic waters from mining activities, the heavy metal ions, sulfate ions colloidal particles difficult to settle are observed in many cases. Particularly, the removal of trace highly toxic metallic ions like Pb(II), Cd(II) and others is a complication mine sites commonly face. The classic process for treating acidic mining solutions only considers a chemical treatment based on contacting the polluted stream with lime (CaO or $Ca(OH)_2$) increasing the pH up to a point where metals precipitate from solution. This process is somehow considered annoying since it produces large amounts of sludge and does not accomplish the complete removal of toxic metals, among other reasons, because of the residual concentrations resulting from their solubility. Furthermore, the precipitate obtained out of this method is often colloidal in nature and, therefore, difficult to separate via standard filtration stages.

Other technical options that can be used to carry out the uptake of pollutants from acidic aqueous solutions are ionic exchange (IX) with solid resins [5,6], solvent extraction (SX) [7], the use of liquid membranes with and without surfactants for extracting and concentrating metal ions from dilute solutions [8,9], solid supported liquid membranes [10,11], biosorption [12,13] and adsorption strategies using natural or synthetic adsorbents such as activated carbon, zeolites, clays and metal oxides [14–16]. Notwithstanding the advantages all the previous mentioned technical options have, they also exhibit disadvantages that inevitably lead toward seeking new and improved wastewater treatment methods.

Specifically, in the field of adsorption many metal oxide adsorbents for removing contaminants from aqueous solutions have been reported. For example, Mustafa et al. [17] studied the use of non-magnetic MnO_2 to remove PO_4^{3-} from aqueous solution reporting good results. Other researchers evaluated the utilization of various compounds such as MnO_2, ZrO_2, Al_2O_3 and SiO_2 to remove Cu(II), Cd(II) and phosphorus species [18–21] while Han et al. [22] presented a study on the adsorption of Cu(II) and Pb(II) using manganese-oxide-coated sand reporting promising results. The metal adsorption capacity of these oxides varies with the solution pH, the initial concentration of the contaminants, the ionic strength of the solution, the particle size of the adsorbent, the zeta potential of the solid phase and the redox potentials of electrochemical reactions taking place in the system. δ-MnO_2 is a common hydrous-oxide adsorbent that can be synthetized in presence of microstructures or nanostructures presenting a large surface area and many OH^- groups that favors the uptake of many ions from aqueous solutions following different adsorption mechanisms [23,24].

However, the most important limitation of using metal oxides as adsorbents is the inherent difficulty of implementing the solid–liquid separation once the adsorption process is finished, mainly because of the colloidal form the oxides present with particle sizes ranging between 0.5 and 5 μm. This research study aims at solving this issue by synthesizing, characterizing and using a magnetized nanostructured metal oxide, which would facilitate the separation of the "pollutants-loaded adsorbents" from the aqueous solutions by using a simple magnetic process.

In a previous report we synthetized a δ-MnO_2 microsorbent for removing trace concentration levels of harmful inorganic contaminants from water [25]. This study moves on toward a next step through synthetizing in a reproducible way a stable nanostructured δ-MnO_2 adsorbent having superparamagnetic properties so as to be used like adsorbent in experiments for removing selected toxic heavy metals (Pb and Cd) from acidic aqueous solutions simulating an AMD from a mine site. Furthermore, the physical and chemical characterization of the synthesized adsorbent is also evaluated and reported.

2. Experimental procedure

2.1. Preparation of the adsorbent δ-MnO_2 with magnetic properties

The synthesis of the adsorbent was carried out in a two-stage sequence. First, magnetite particles were prepared using coprecipitation of Fe(II) and Fe(III) salts, according to a method described in previous studies [26]. In a beaker, under nitrogen inert atmosphere and at room temperature, 50 mL of $FeCl_3$ 0.2 M and 50 mL of $FeCl_2$ 0.1 M were mixed. Afterward, the temperature was increased until 80°C where 10 mL of a concentrate solution of NH_4OH was added reaching a pH close to 9.0. The black magnetite particles were readily formed being separated magnetically from the aqueous solution using a magnet. After washing these particles, the solid obtained was divided into two representative subsamples. One subsample was washed and dried at 40°C while the other was kept in a 0.01 M $NaNO_3$ solution.

Second, the magnetic δ-MnO_2 adsorbent was prepared using an oxidative precipitation method in alkaline medium, consisting of the oxidation of Mn(II) ions caused by the presence of $KMnO_4$ as oxidizing agent, according to the following chemical reaction:

$$3MnCl_{2(aq)} + 2KMnO_{4(aq)} + 4OH^-_{(aq)} \rightarrow 5MnO_{2(s)} + 2K^+_{(aq)} + 6Cl^-_{(aq)} + 2H_2O_{(l)} \quad (1)$$

In order to obtain a manganese oxide with magnetic properties, the synthesis of δ-MnO_2 was performed in presence of magnetite (Fe_3O_4), previously prepared. Different MnO_2/Fe_3O_4 proportions were prepared and evaluated. The addition of KOH permitted to reach pH 12. The suspension was mechanically stirred at 500 rpm during 30 min. A dark-brownish solid was rapidly obtained and separated from the solution by using a neodymium magnet. The product was then washed with distilled water. A representative subsample was obtained and dried at 100°C. The rest was kept in a 0.01 M $NaNO_3$ solution to study its stability. In order to compare the characteristics of the adsorbent synthesized under different experimental conditions, in other separate experiments, the MnO_2/Fe_3O_4 adsorbents were prepared using a similar process but in acid medium following a slightly modified method with respect to one found in the literature [27].

2.2. Characterization of the adsorbent

The magnetic δ-MnO_2 particles were characterized employing several analytical techniques. They were analyzed using scanning electron microscopy (SEM) and transmission electron microscopy (TEM) using an SEM FEI INSPECT F50 apparatus. The specific surface area of the particles was

determined via BET measurements using a N_2 sorptometer at 77 K in a Micromeritics ASAP 2010 device.

The zeta potential of the particles was measured by using a Malvern Mastersizer Hydro 2000 MU, Malvern Instrument Ltd., UK, microelectrophoresis device at different pH values. Aqueous solutions of 0.1 M HNO_3 and 0.1 M NaOH were used as pH modifiers. In the same way, the determination of the particle size distribution was conducted by using a dynamic light scattering in a Malvern MasterSizer HYDRO 2000MU equipment. For determining the particle size distribution, adsorbent samples were suspended in a 0.01 M $NaNO_3$ solution. The particles were also analyzed by using X-ray powder diffraction (XRD) technique in a Bruker D8 ADVANCE device.

The magnetic properties of the magnetic δ-MnO_2 particles were measured by means of vibrating sample magnetometer. The manganese and iron contents in the adsorbent and all the metal concentrations in aqueous solutions were determined by atomic absorption spectrometry (AAS) technique using a PerkinElmer PinAAcle 900F apparatus. When necessary, inductively coupled plasma mass spectrometry (ICP–MS) was used for determining lower concentrations of heavy metals dissolved in solutions.

2.3. Adsorption and adsorbent stability experiments

Before carrying out the adsorption experiments, a series of preliminary experimental runs were conducted to verify the chemical stability of the synthesized adsorbent via solubility tests. The solubility of the adsorbent was evaluated as follows: 50 mg of the adsorbent MnO_2:Fe_3O_4 (1:1) were contacted with 50 mL of aqueous solutions with initial pH values between 2 and 7 at 25°C in an orbital shaker during 24 h. The pH of the acid solutions was adjusted using 0.1 M H_2SO_4 and/or 0.1 M NaOH. Once finalizing the solubility experiments, the aqueous solutions were submitted to chemical analyses to measure the Mn and Fe concentrations using AAS technique. Identical chemical analyses were performed to the solids residues.

Pb(II) and Cd(II) adsorption experiments were conducted separately at different pH values. These experiments were carried out at 25°C by contacting 50 mg of the MnO_2:Fe_3O_4 (1:1) adsorbent with 250 mL of the corresponding single-metal aqueous solutions containing in all cases an initial metal concentration of 10 mg/L. Furthermore, for each one of the metals, Pb(II) and Cd(II), adsorption equilibrium and kinetics tests were performed by contacting a fixed mass of the same adsorbent with aqueous solutions having different initial metal concentrations. The initial pH was adjusted at 4.0 in all cases, and the solid–liquid mixtures were placed in a Polyscience orbital shaker apparatus at 25°C.

3. Results and discussion

3.1. Synthesis

The magnetite ($FeO{\cdot}Fe_2O_3$) was synthesized via the coprecipitation of Fe(II) and Fe(III) salts method in alkaline conditions. The synthesis was fast, efficient and reproducible with a yield over 90%. In the same way, the preparation of the adsorbent in its final stage was also quick and quantitative obtaining a dark-brownish solid associated with MnO_2. At this stage, the oxidative precipitation of Mn(II) ions was performed in presence of magnetite particles previously synthesized. Considering the yield of manganese oxide, different MnO_2:Fe_3O_4 ratios were tested, namely 1:2, 1:1 and 2:1. From their chemical stability, magnetic behavior and the results of the preliminary adsorption experiments, the MnO_2:Fe_3O_4 (1:1) was stablished as the best experimental condition. In this case, the solid presents an average composition of 10.6% Mn and 37.7% Fe exhibiting a suitable surface area available for adsorption processes and magnetic properties strong enough for assuring an effective separation from the aqueous solution once the adsorption process finishes.

3.2. Characterization of the adsorbent

Fig. 1 shows an SEM image of the magnetic δ-MnO_2 adsorbent. A clear crystalline structure is observed, caused mainly by the magnetite since the manganese oxide is amorphous. The formation of particle agglomerates with an average size of a few microns consisting of particles with sizes below 1 μm was also observed. Fig. 2 shows a TEM photograph.

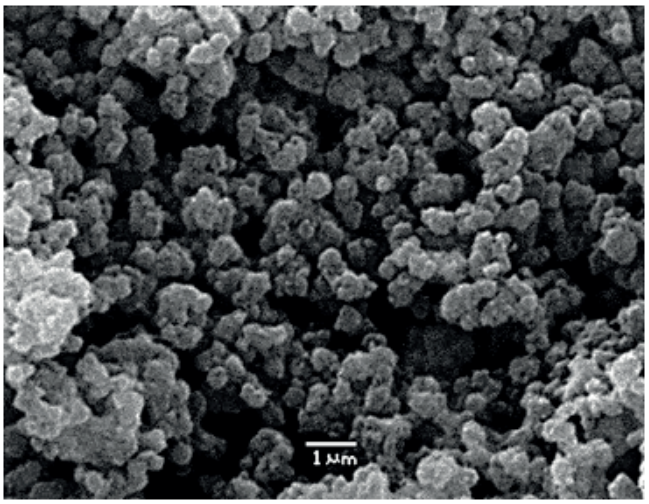

Fig. 1. SEM micrograph of nanomagnetic MnO_2 adsorbent.

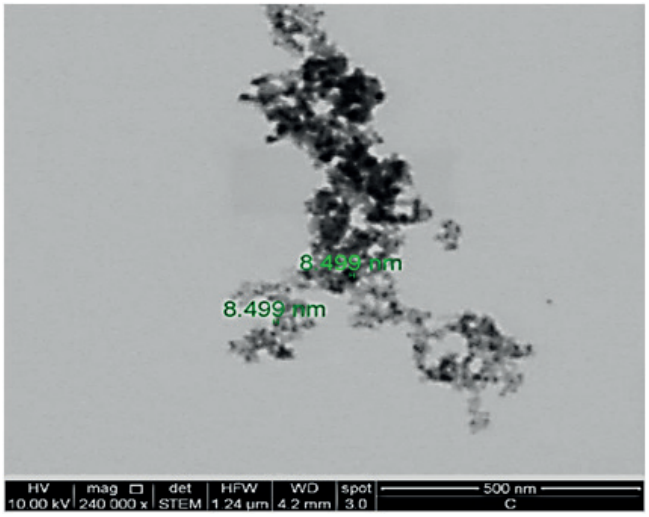

Fig. 2. TEM image of nanomagnetic MnO_2 adsorbent.

Aggregates of almost spherical particles where the dark zone corresponds to the magnetite nucleus surrounded by clearer amorphous layer of manganese oxide are observed. The image also shows that the agglomerates are constituted by individual particles with diameters between 6 and 9 nm, confirming that the synthesized particles of the adsorbent are clearly nanoparticles, much smaller than those obtained before which were just microparticles [25].

BET analysis indicated that the magnetite (Fe_3O_4) has a specific surface area of 93 m^2/g and the adsorbent showed an average value of 90 m^2/g, ensuring a significant surface area for the adsorption process. The particle size distribution results showed a unimodal-like and narrow distribution between 105 and 120 nm presenting a maximum at 110 nm. This measurement was done in an aqueous solution (0.01 M $NaNO_3$) where the agglomeration of the particles may have occurred as a higher particle size than that determined by TEM analysis is observed.

Fig. 3 presents XRD analysis results of the adsorbent synthesized in alkaline and in acid media as well as that of the magnetite. Both diffractograms are almost identical. The signals found at 2θ of 30°, 35°, 44°, 57° and 63° correlate well with the crystalline structure of Fe_3O_4. Peaks corresponding to δ-MnO_2 are not observed confirming its amorphous structure. Manganese oxide would build up and adhere to the magnetite nucleus forming an external layer of a few nanometers thickness. However, authors have indicated that Mn would also be partially incorporated into magnetite structure by replacing some Fe ions in the magnetite lattice producing an expansion of the crystalline structure due to its larger ionic radius [28].

Considering the importance of the magnetic properties of the synthesized composite, the magnetization curves of magnetite and δ-MnO_2 were obtained. Fig. 4 presents the variation of the magnetic saturation (Ms) expressed in emu/g as a function of the applied magnetic field expressed in Oe (1 emu/g = 10 k Oe). As expected, δ-MnO_2 practically does not present any degree of magnetization.

The magnetic response of differently prepared composites indicates that the Ms decreases when increasing the δ-MnO_2 content in the adsorbent (Fig. 4 and Table 1). The reduction of the magnetization would occur because during the synthesis of manganese oxide, some of the Fe atoms present in the Fe_3O_4 structure would effectively be replaced by Mn ions producing a less crystalline structure with lower magnetic properties. Consequently, a composite consisting of MnO_2:Fe_3O_4 (2:1) presented a low degree of magnetization making unfeasible the complete separation of the loaded adsorbent from the aqueous solution raffinate.

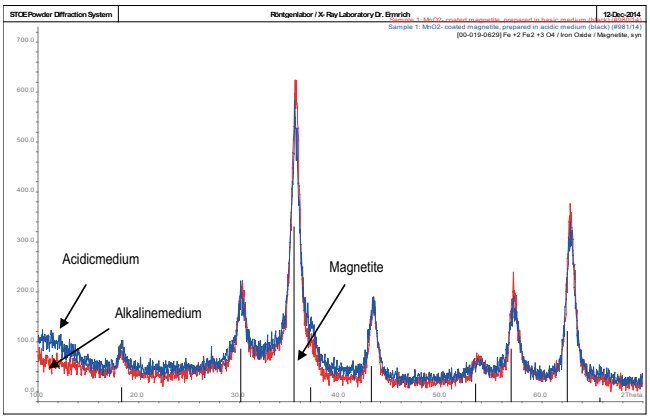

Fig. 3. XRD patterns of nanomagnetic MnO_2 adsorbent and magnetite.

The highest magnetization was obtained with the sample of magnetite synthesized in this study (around 57 emu/g). This value is smaller than those reported in other studies, which would be due to the fact that during the synthesis under strong oxidative conditions, part of the Fe^{2+} would be oxidized to Fe^{+3} generating maghemite-like structure (Fe_2O_3), which possess a lower value of Ms. However, most of the adsorbents prepared in this study showed suitable magnetic properties to remove the loaded-pollutant particles from the aqueous solution using a simple magnet. Examples of this are the magnetic δ-MnO_2 adsorbents synthesized using manganese oxide/magnetite proportions equal to MnO_2:Fe_3O_4 (1:1) and MnO_2:Fe_3O_4 (1:2), as shown in Fig. 4. The higher the weight percentage of magnetite in the adsorbent, the higher the Ms reached. Moreover, the adsorbent composites presented superparamagnetic characteristics having almost a null coercivity, which could allow reusing the magnetic particles in subsequent wastewater treatment cycles.

The zeta potential of the adsorbent composite was measured as a function of pH. The point of zero charge (pH_{PZC}) of the MnO_2:Fe_3O_4 (1:1) surface is around pH 3.5, which might determine the charge of the ionic species that predominantly would be adsorbed. Below this value the surface of the magnetic adsorbent would be highly protonated enhancing the adsorption of anionic species by ion-pair formation. On the contrary, when the pH of the polluted solution is above

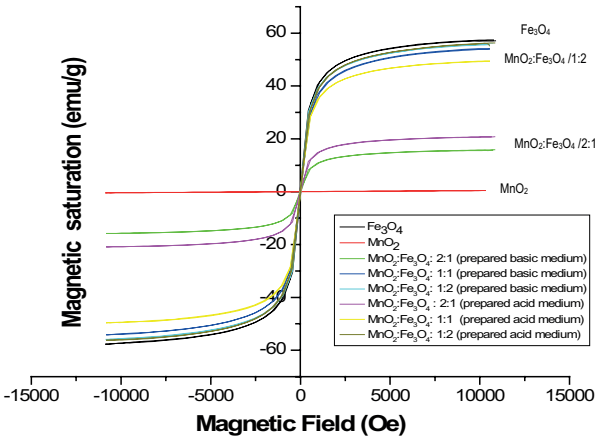

Fig. 4. Magnetization curves of adsorbents, MnO_2 and Fe_3O_4.

Table 1
Values of magnetic saturation (Ms) of adsorbents synthesized in basic medium and magnetization of prepared magnetite

Material	Ms (emu/g)
Sorbent, MnO_2:Fe_3O_4 (2:1)	15.84
Sorbent, MnO_2:Fe_3O_4 (1:2)	56.08
Fe_3O_4	57.07

the point of zero charge, the protonation of surface groups is weaker. Under this condition, the adsorption of heavy metal cations would be favored by means of cation-exchange mechanisms, by releasing H^+ to the raffinate solution. In addition, the pH_{PZC} of the magnetite was close to pH 6.0, which limits its capability for undertaking the adsorption of cationic species.

3.3. Adsorbent stability measurements and adsorption experiments

One of the most interesting applications of these magnetic adsorbents is their employment for removing low contents of toxic heavy metals and metalloids from acidic waters from mining activities. Then, it is important to verify the chemical stability of the adsorbent as a function of the level of acidity the wastewaters may exhibit. This aspect is also important for evaluating the reutilization of the adsorbent in subsequent adsorption cycles. The latter may be achieved by using sorbents that assure a good reversibility for the adsorption process. Samples of the synthesized adsorbent MnO_2:Fe_3O_4 (1:1) prepared in alkaline conditions were contacted with aqueous solutions with pH values between 2.0 and 7.0. Results are shown in Table 2.

The leach of Mn and Fe were very low in this range of pH, and as expected, the dissolution of both metals from the adsorbent increased with the level of acidity of the aqueous solution. Leaching of manganese and iron in the most acidic pH conditions tested would result from the interaction between the metal oxides and the high concentration of hydrogen ions present in the solution triggering a cation exchange mechanisms that would release Mn and/or Fe ions into aqueous raffinate.

In order to test the capability of the synthesized adsorbent to remove heavy metals from acidic aqueous solutions, a set of preliminary experiments were carried out using the magnetic adsorbent prepared in alkaline medium. One of the main variables that would affect the adsorption is the initial pH of the treated solution. In principle, the pH of the solution would determine the electric charge of the sorbent surface. The adsorbent (S_M) is a hydrous-oxide compound, and therefore, its surface may undergo protonation or deprotonation reactions as shown in the following equations generating positive, negative or neutral surface charge.

$$S_M - OH + H^+ \leftrightarrow S_M - OH_2^+ \quad (2)$$

$$S_M - OH + OH^- \leftrightarrow S_M - O^- + H_2O \quad (3)$$

$$S_M - OH \leftrightarrow S_M - O^- + H^+ \quad (4)$$

Table 2
Chemical stability tests of nanomagnetic adsorbent as a function of the acidity of aqueous solution: adsorbent – MnO_2:Fe_3O_4 (1:1)

Initial pH aqueous solution	2.35	3.17	4.25	5.71	6.23	7.07
Mn dissolution (%)	0.082	0.073	0.068	0.063	0.060	0.046
Fe dissolution (%)	2.510	0.021	0.014	0.019	0.018	0.015

Fig. 5 shows the adsorption percentage of Pb(II) and Cd(II) ions for pH conditions ranging from 3 to 6. The adsorption of both ions, studied separately in this research work, increased with the pH of the aqueous solution. The adsorption of the cationic species was favored at pH values above the point of zero charge, which is in agreement with the measured pH_{PZC} (around 3.5). Under this pH condition, a cationic exchange of the dissolved metal (e.g., Pb^{2+}) with the hydrogen ions present at the surface sites occurs as follows:

$$S_M - OH_{(ad)} + Pb^{2+}{}_{(aq)} \leftrightarrow S_M - OPb^+{}_{(ad)} + H^+{}_{(aq)} \quad (5)$$

$$2S_M - OH_{(ad)} + Pb^{2+}{}_{(aq)} \leftrightarrow (S_M - O)_2\, Pb_{(ad)} + 2H^+{}_{(aq)} \quad (6)$$

where S_M represents the hydrous-oxide adsorbent, and the subscripts ad and aq indicate whether the radical is placed on the surface of the adsorbent or in the aqueous solution, respectively.

Higher adsorption efficiencies are observed at higher pH values that can be explained due to the strong dissociation of OH^- groups (as it is shown in Eq. (4)) releasing a higher number of exchangeable protons with the metal cations. Fig. 5 indicates that the ion-exchange capacity of the MnO_2-magnetic adsorbent for Pb(II), observed in these preliminary adsorption experiments, is higher than that measured for Cd(II). The latter could be due to the small hydrated ionic diameter of Pb(II) ions compared with that of cadmium ions, which may enhance its adsorption. However, this consideration must be studied into more detail in order to get a more reliable conclusion. For instance, the type and stability of metal complexes could be more important than the size of the hydrated radii of ions in solution.

Additionally, it is also important to verify the possibility to recycle the adsorbent for subsequent adsorption–desorption cycles. In this sense, desorption tests of Pb(II)-loaded

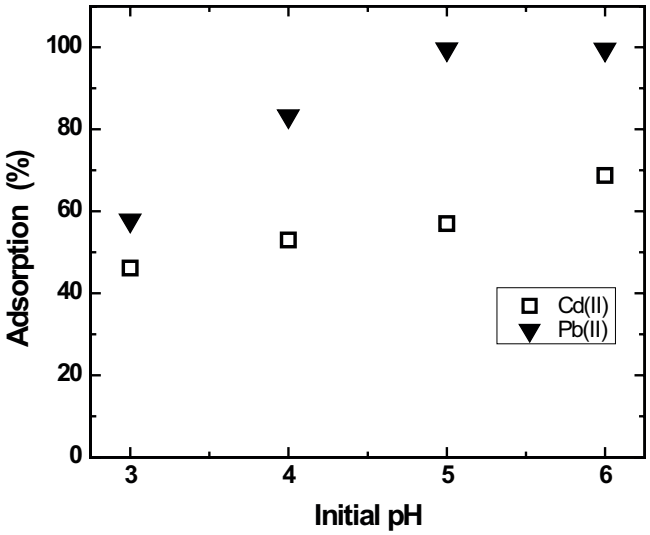

Fig. 5. Dependence of Pb(II) and Cd(II) ions adsorption onto magnetic adsorbent with initial pH: (experimental conditions: adsorbent 50 mg, aqueous solution 250 mL, metal content 10 mg/L).

adsorbent were conducted using an initial pH equal to 3.5 and aqueous solution as desorption medium. The resulting unloaded adsorbent was used again in repetitive cycles by contacting it with new fresh aqueous solutions containing 10 mg/L Pb(II) having an initial pH 6.0. The efficiency of the desorption process was almost quantitative averaging a 98%, after five adsorption–desorption cycles. In turn, the adsorption capability of the regenerated adsorbent slightly diminished accordingly to the desorption degree. However, the readsorption ability of the adsorbent can be improved using a desorption solution with higher levels of acidity so as to promote the metal desorption from the δ-MnO_2 surface without losing the nanostructure of the adsorbent and avoiding its partial dissolution. These results confirm that the removal of low contents of toxic metals from acid aqueous solutions should be a specific target for using this sort of adsorbents, which presents promising results to treat acid wastewaters.

3.4. Adsorption Equilibrium

Adsorption equilibrium studies of Pb(II) and Cd(II) onto the nanostructured-magnetic-δ-MnO_2 adsorbent from acid aqueous solutions were performed. Experimental results were analyzed using different equilibrium isotherms including the hybrid Redlich–Peterson, Langmuir and Freundlich adsorption isotherms. The Langmuir and Freundlich isotherms explained adequately the experimental results. The well-known Langmuir isotherm corresponds to a monolayer-type adsorption model over a homogeneous surface. It assumes that all the adsorption sites exhibit the same shape and heat of adsorption and is expressed as follows:

$$q_e = \frac{q_m \cdot K_L \cdot C_e}{1 + K_L \cdot C_e} \tag{7}$$

In turn, the Freundlich isotherm model depicts an empirical model based on multilayer-type adsorption on heterogeneous surfaces and is expressed as follows:

$$q_e = K_F \cdot C_e^{1/n_F} \tag{8}$$

In these equations q_e denotes the amount in mmol g^{-1} adsorbed at equilibrium; q_m is the amount of adsorbate required to fully cover the adsorbent surface mmol g^{-1}; K_L is Langmuir's constant in L $mmol^{-1}$ and C_e is the metal concentration in mmol L^{-1} that remains in solution after the adsorbate extraction. Furthermore, n is a dimensionless constant related to the intensity of the adsorption, and K_F is the Freundlich constant commonly associated to the adsorption capacity in L^{-n} $mmol^{-n}$. The parameters were evaluated by using the Levenberg–Marquardt method commonly applied in non-linear least-squares problems [29].

Figs. 6 and 7 show the adsorption equilibria of Pb(II) and Cd(II) onto the MnO_2:Fe_3O_4 (1:1) adsorbent, and Tables 3 and 4 show the calculated values of the parameters for Langmuir and Freundlich isotherms, respectively. Analysis of χ^2 reveals that, in general, both equilibrium isotherm models are in good agreement with the experimental results. In all cases the values of χ^2 proved to be very

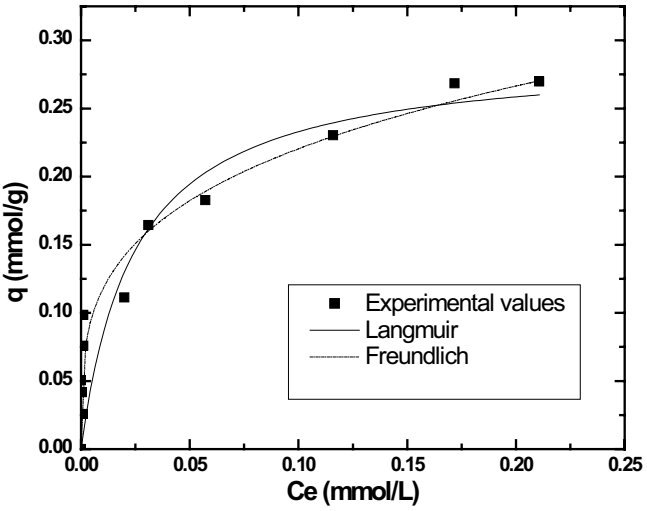

Fig. 6. Adsorption equilibrium of Pb(II) using the nanomagnetic MnO_2 adsorbent.

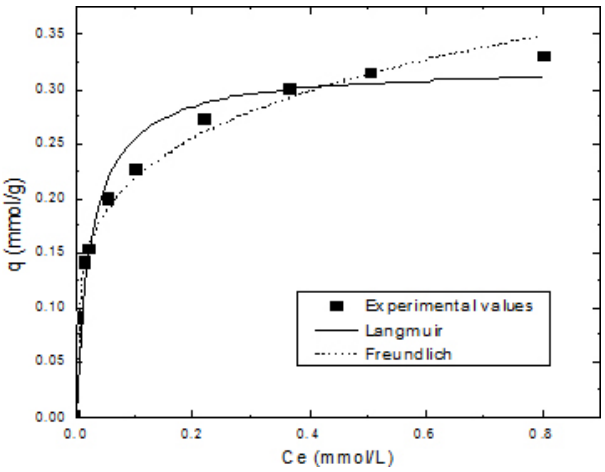

Fig. 7. Adsorption equilibrium of Cd(II) using the nanomagnetic MnO_2 adsorbent.

Table 3
Parameters of the Langmuir equilibrium model for the adsorption of Pb(II) and Cd(II) using nanomagnetic MnO_2 adsorbent

	q_m (mmol/g)	K_L (L/mmol)	χ^2 (mmol/g)	R^2
Pb(II)	0.29 ± 0.04	40.5 ± 23.1	1.69×10^{-3}	0.81
Cd(II)	0.32 ± 0.01	37.8 ± 6.5	3.73×10^{-4}	0.92

Table 4
Parameters of the Freundlich equilibrium model for the adsorption of Pb(II) and Cd(II) using nanomagnetic MnO_2 adsorbent

	K_F (L^{-n} $mmol^{-n}$]	n_F	χ^2 (mmol/g)	R^2
Pb(II)	0.41 ± 0.03	3.66 ± 0.39	4.25×10^{-4}	0.94
Cd(II)	0.37 ± 0.01	4.43 ± 0.41	3.62×10^{-4}	0.98

small indicating a reduced error between the experimental data and those calculated using the model. Nevertheless, the high standard deviation of the calculated values of the Langmuir constants for both ions allows us stating that the Freundlich isotherm is more reliable and valid. Then, it is possible to indicate that the adsorption of Pb(II) and Cd(II) ions, under the experimental conditions employed in this study, would follow a non-ideal multilayer-type adsorption isotherm.

3.5. Adsorption kinetics

Adsorption kinetic tests were conducted using aqueous solutions containing Cd(II) and Pb(II) ions. The pH was adjusted at 4.0 as well as the ionic strength by adding 0.01 M $NaNO_3$. The experiments were carried out using 50, 100 and 200 mg of the MnO_2:Fe_3O_4 (1:1) adsorbent and 10 mg/L metal initial concentration. Figs. 8 and 9 show the results for Pb(II) and Cd(II), respectively.

In general, the adsorption is high and almost quantitative in many cases. It is observed that Pb(II) adsorption kinetics is faster than that of Cd(II). The experimental results were fitted using different kinetics models. Particularly, a pseudo-second-order adsorption kinetic model explained well the experimental data. This model depends more on the adsorptive capability of the adsorbent than on the concentration of the adsorbate in the aqueous solution. The model describes how the adsorption active sites disappear with time according to the following differential equation [30,31].

$$\frac{dq_t}{dt} = -k\left(q_e - q_t\right)^2 \tag{9}$$

where q_e and q_t correspond to the amount of metal ions adsorbed at equilibrium and at a time t, respectively; both expressed in mg metal/g sorbent, while k represents the adsorption specific rate constant. Integrating the previous equation considering the following boundary conditions: $q_t = 0$ for $t = 0$ and $q_t = q_t$ for $t = t$; the following linearized expression is obtained:

$$\frac{t}{q_t} = \frac{1}{kq_e^2} + \frac{1}{q_e t} \tag{10}$$

Fig. 10 shows the results when the experimental values of Pb(II) and Cd(II) adsorption on the composite adsorbent MnO_2:Fe_3O_4 are arranged according to Eq. (10), in experiments conducted using 50 mg of adsorbent. The q_e values are 9.8 and 10.4 mg/g adsorbent for Pb(II) and Cd(II), respectively. These q_e values calculated using the kinetic model agree well with those obtained experimentally. On the other hand, specific rate constants of 0.8947 and 0.4381 g/mg min were determined for the adsorption of Pb(II) and Cd(II), respectively. These values are higher than those informed by other authors who prepared the adsorbent in an acid medium obtaining bigger particles with a mean diameter of 60 nm, compared with ours synthesized in an alkaline medium having a diameter between 6 and 9 nm [27].

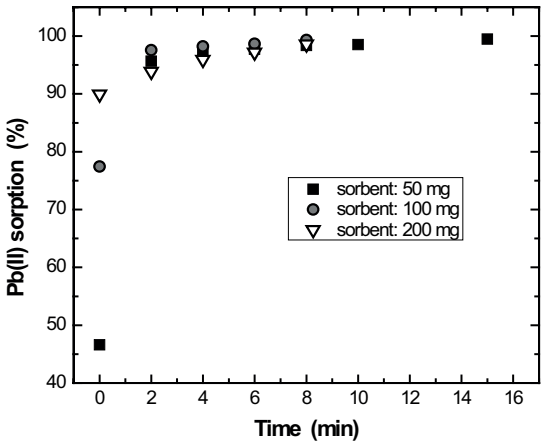

Fig. 8. Adsorption of Pb(II) as a function of the mass of adsorbent and time: (experimental conditions: aqueous solution 50 mL, metal content 10 mg/L, pH 4.0).

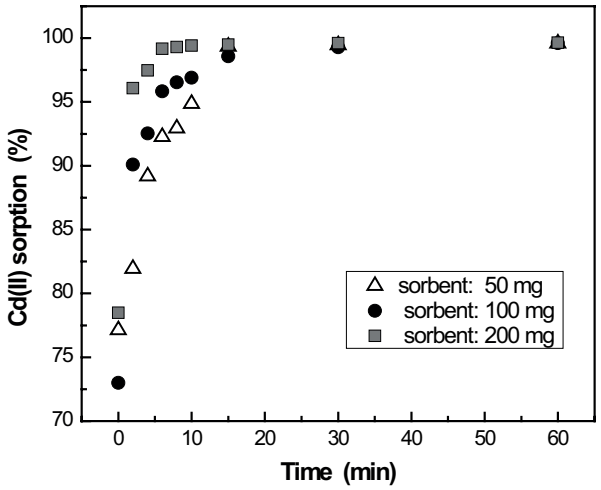

Fig. 9. Adsorption of Cd(II) as a function of the mass of adsorbent and time: (experimental conditions: aqueous solution 50 mL, metal content 10 mg/L, pH 4.0).

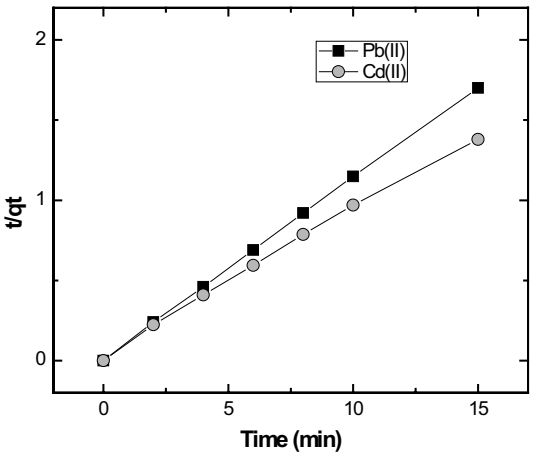

Fig. 10. Pseudo-second-order kinetics model for the adsorption of Pb(II) and Cd(II) onto nanomagnetic MnO_2 adsorbent.

4. Conclusions

Nanoparticles of an adsorbent with magnetic properties based on Fe_3O_4 coated with δ-MnO_2 were successfully synthesized. The nanostructure of the composite and its significant surface area full of vacant adsorption sites permit a fast and efficient adsorption of many metal ionic species existing in aqueous solutions. The adsorption capability of this composite depends on the acidity of the treated aqueous solution. The adsorbent exhibits a point of zero charge around 3.5. Above this pH value, the adsorption of cationic species is enhanced following an ion-exchange reaction between the metal in solution and the hydrogen ions dissociated from the surface of the hydrous-oxide adsorbent.

The adsorbent composite showed a magnetic moment of 54 emu/g, smaller than that of magnetite; however, the magnetic properties are adequate to ensure the complete separation of the pollutant-loaded adsorbent particles from the aqueous raffinate, which is the main goal of this study. The adsorbent is fairly stable even at pH values close to 2.0 where only a very low dissolution of Mn and Fe was observed. Adsorption equilibrium results are correctly explained by the Freundlich isotherm and adsorption kinetic data fit well with a pseudo-second-order model.

Acknowledgment

The authors gratefully acknowledge the support given by Chile-FONDECYT through the research grant No. 1140331.

References

[1] D. Johnson, K. Hallberg, Acid mine drainage remediation options: a review, Sci. Total Environ., 338 (2005) 3–14.
[2] F. Valenzuela, C. Araneda, F. Vargas, C. Basualto, J. Sapag, Liquid membrane emulsion process for recovering the copper content of a mine drainage, Chem. Eng. Res. Des., 87 (2009) 102–108.
[3] T. Chen, B. Yan, C. Lei, X. Xiao, Pollution control and metal resource recovery for acid mine drainage, Hydrometallurgy, 147 (2014) 112–119.
[4] Norm, N° 90/2000, Maximum Allowable Limits for Discharge of Liquid Wastes to Continental and Marine Surface Waters, Minister of General-Secretary of Presidence, Chile Government, 2001.
[5] A. Dabrowski, Z. Hubicki, P. Podkoscielny, E. Robens, Selective removal of the heavy metal ions from waters and industrial wastewaters by ion-exchange method, Chemosphere, 56 (2004) 91–106.
[6] C. Rokicki, T. Boyer, Effect of divalent metal cations on contaminant removal by bicarbonate-form anion exchange resin, Sep. Sci. Technol., 50 (2015) 2284–2294.
[7] A. Guimaraes, P. da Silva, M. Mansur, Purification of nickel from multicomponent aqueous sulfuric solutions by synergistic solvent extraction using Cyanex 272 and Versatic 10, Hydrometallurgy, 150 (2014) 173–177.
[8] F. Valenzuela, C. Basualto, J. Sapag, J. Romero, W. Höll, C. Fonseca, C. Araneda, A kinetics analysis applied to the recovery of Zn(II) content from mine drainage by using a surfactant liquid membrane, Desal. Wat. Treat., 24 (2010) 327–335.
[9] M. García, A. Acosta, J. Marchese, Emulsion liquid membrane pertraction of Cr(III) from aqueous solutions using PC-88A as carrier, Desalination, 318 (2013) 88–96.
[10] C. Kedari, S. Pandit, P. Gandhi, Separation by competitive transport of uranium(VI) and thorium(IV) nitrates across supported renewable liquid membrane containing trioctylphosphine oxide as metal carrier, J. Membr. Sci., 430 (2013) 188–195.
[11] K. Bhatluri, M. Manna, P. Saha, A. Ghoshal, Supported liquid membrane-based simultaneous separation of cadmium and lead from wastewater, J. Membr. Sci., 459 (2014) 256–263.
[12] D. Cotorás, F. Valenzuela, M. Zarzar, P. Viedma, Process for the Removal of Metals by Biosorption from Mining or Industrial Effluents, US Patent 7326344, 2008.
[13] B. Cayllahua, M. Torem, Biosorption of aluminum ions onto *Rhodococcus opacus* from wastewaters, Chem. Eng. J., 161 (2010) 1–8.
[14] K. Gedik, I. Imamoglu, Affinity of clinoptilolite-based zeolites towards removal of Cd from aqueous solutions, Sep. Sci. Technol., 43 (2008) 1191–1207.
[15] B. Olu-Owolabi, D. Popoola, E. Unuabonah, Removal of Cu(II) and Cd(II) from aqueous solution by bentonite clay modified with binary mixture of goethite and humic acid, Water Air Soil Pollut., 211 (2010) 459–474.
[16] G. Montes-Atenas, F. Valenzuela, S. Montes, The application of diffusion-reaction mixed model to assess the best experimental conditions for bark chemical activation to improve copper(II) ions adsorption, Environ. Earth Sci., 72 (2014) 1625–1631.
[17] S. Mustafa, M. Zaman, S. Khan, pH effect on phosphate sorption by crystalline MnO_2, J. Colloid Interface Sci., 301 (2006) 370–375.
[18] F. Long, J. Gong, G. Zeng, L. Chen, X. Wang, J. Deng, Q. Niu, H. Zhang, X. Zhang, Removal of phosphate from aqueous solution by magnetic Fe–Zr binary oxide, Chem. Eng. J., 171 (2011) 448–455.
[19] M. Anbia, Z. Ghassemian, Removal of Cd(II) and Cu(II) from aqueous solutions using mesoporous silicate containing zirconium and iron, Chem. Eng. Res. Des., 89 (2011) 2770–2775.
[20] M. Somayeh, J. Mohsen, Effect of TiO_2, Al_2O_3, and Fe_3O_4 nanoparticles on phosphorus removal from aqueous solution, Environ. Prog. Sustain. Energy, 33 (2014) 1209–1219.
[21] S. Brijesh, C. Uma, Synthesis and characterization of a novel hybrid material as amphoteric ion exchanger for simultaneous removal of cations and anions, J. Hazard. Mater., 276 (2014) 138–148.
[22] R. Han, L. Zhu, W. Zou, D. Wang, J. Shi, J. Yang, Removal of copper(II) and lead(II) from aqueous solution by manganese oxide coated sand: II. Equilibrium study and competitive adsorption, J. Hazard. Mater., 137 (2006) 480–488.
[23] P. Julius-Pretorius, P. Linder, The adsorption characteristics of δ-manganese dioxide: a collection of diffuse double layer constants for the adsorption of H^+, Cu^{2+}, Ni^{2+}, Zn^{2+}, Cd^{2+} and Pb^{2+}, Appl. Geochem., 16 (2001) 1067–1082.
[24] S. Ahmadi, N. Akbari, Z. Shiri-Yekta, M. Mashhadizadeh, A. Pourmatin, Adsorption of strontium ions from aqueous solution using hydrous, amorphous MnO_2–ZrO_2 composite: a new inorganic ion exchanger, J. Radioanal. Nucl. Chem., 299 (2014) 1701–1707.
[25] C. Calderón, M. Franzreb, F. Valenzuela, W. Höll, Magnetic manganese dioxide as an amphoteric adsorbent for removal of harmful inorganic contaminants from water, React. Funct. Polym., 70 (2010) 516–520.
[26] C. Basualto, J. Gaete, L. Molina, F. Valenzuela, C. Yañez, J. Marco, Lanthanide sorbent based on magnetite nanoparticle functionalized with organophosphorus extractants, Sci. Technol. Adv. Mater., 16 (2105) 035010. doi: 10.1088/1468-6996/16/3/035010
[27] E. Kim, C.-S. Lee, Y.-Y. Chang, Y.-S. Chang, Hierarchically structured manganese oxide-coated magnetic nanocomposites for the efficient removal of heavy metal ions from aqueous systems, ACS Appl. Mater. Interfaces, 5 (2013) 9628–9634.
[28] C. Warner, W. Chouyyok, K. Mackie, D. Neiner, L. Saraf, T. Droubay, M. Warner, R. Addleman, Manganese doping of magnetic iron oxide nanoparticle: tailoring surface reactivity for a regenerables heavy metal sorbent, Langmuir, 28 (2012) 3931–3937.
[29] Y. Ho, Selection of optimum sorption isotherm, Carbon, 42 (2004) 2115–2116.
[30] Y. Ho, Review of second-order models for adsorption systems, J. Hazard. Mater., 136 (2006) 681–689.
[31] G. Barassi, A. Valdés, C. Araneda, C. Basualto, J. Sapag, C. Tapia, F. Valenzuela, Cr(VI) sorption behaviour from aqueous solutions onto polymeric microcapsules containing a long-chain quaternary ammonium salt: kinetics and thermodynamics analysis, J. Hazard. Mater., 172 (2009) 262–268.